WEAKLY SHEARED ACTIVE SUSPENSIONS OF RIGID ELLIPSOIDS

By

Zhenlu Cui

IMA Preprint Series # 2321

(June 2010)

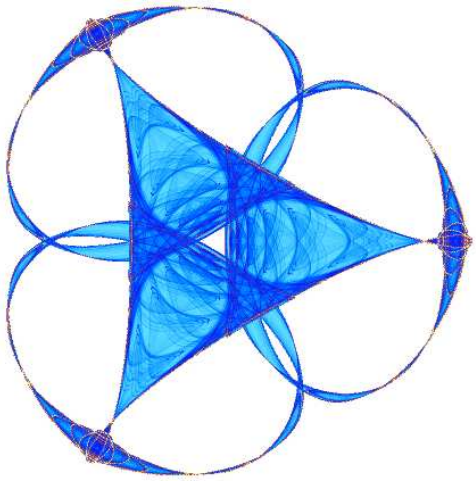

INSTITUTE FOR MATHEMATICS AND ITS APPLICATIONS

UNIVERSITY OF MINNESOTA

400 Lind Hall
207 Church Street S.E.
Minneapolis, Minnesota 55455–0436

Phone: 612-624-6066 Fax: 612-626-7370
URL: http://www.ima.umn.edu

Weakly Sheared Active Suspensions of Rigid Ellipsoids

Zhenlu Cui
Department of Mathematics and Computer Science
Fayetteville State University, Fayettevill, NC, USA 28301

We present a kinetic model for active suspensions and analyze the behavior of a suspension subjected to slow steady simple shear. We give the stability analysis of the steady states and predict the rheology of such systems including an activity thickening or thinning behavior of the apparent viscosity and a negative apparent viscosity depending on the particle type, their flow alignment behavior, and the boundary anchoring conditions of the director, which can be tested on bacterial suspensions.

PACS numbers: 87.16.A-, 87.10.Ed, 83.80.Xz

I. INTRODUCTION

Recently there has been considerable interest [1–8] in understanding the dynamics and rheology of active particle suspensions, such as bacterial swimmers [6, 9, 10], cell extracts and motor proteins [11]. Such systems differ from their passive counterparts in that particles absorb energy and generate motion. Due to their anisotropic shape, active particles can exhibit orientational order and form nematic phases, characterized by a macroscopic axis of mean orientation identified by a unit vector $\mathbf{n}$ and global symmetry for $\mathbf{n} \rightarrow -\mathbf{n}$, likened to "living liquid crystals" [12] or active liquid crystals. Properties of these self-organizing systems are of fundamental interest to potential technological applications [13].

Conventional liquid crystals exhibit a rich dynamic behavior when subject to external forcing, such as shear or applied magnetic and electric fields. This includes phase transitions, shear banding [14], and even the turbulent and chaotic behavior in the presence of shear [15]. Activity imparts non-trivial physical properties and leads to striking phenomena such as bacterial swarming [16] and the spontaneous flow even in the absence of externally applied forces, both stationary and oscillatory [3, 4, 7, 8], in sharp contrast to their passive counterparts. It is not surprising that the rheology of such active liquid crystals in response to an external shear will be very rich.

Hatwalne et al [1] first generalized continuum theory for liquid crystals to model the rheology of active suspensions and pointed out that activity lowers the viscosity of tensile suspensions (pushers) such as most swimming bacteria, while it enhances the viscosity of contractile systems (pullers) such as Chlamydomonas. Later, Liverpool and Marchetti [2] presented a microscopic model of contractile suspensions of motor-filaments mixtures and confirmed these results and predicted an actual divergence of the viscosity of contractile suspensions at the transition. Cates et al [17] conducted numerical studies of active nematic films and confirmed that this result survives when the effect of boundaries is included. Sokolov et al [18] measured the microrheology of suspensions of pusherlike bacteria (Bacillus subtilis) and demonstrated reduction of viscosity in suspension of swimming bacteria. Rafaï et al [19] have experimentally shown that active suspensions of puller-type microswimmers Chlamydomonas present a dramatic increase in effective viscosity.

Kinetic theories have long been used to study suspensions of rodlike or disclike particles [20–22]. Recently, Saintillan [6] used a simple kinetic theory to study the rheology of a dilute slender suspension of self-propelled particles in a shear flow. He showed that suspensions of pullers exhibit increased viscosity compared to passive suspensions, while pusher suspensions exhibit a significant decrease in viscosity due to the activity; these results are consistent with previous predictions of Hatwalne et al [1]. However, the model is homogeneous, hydrodynamic interactions are not taken into account. Understanding of the complex dynamics and rheology of active suspensions requires exploring the full parameter space, including liquid crystalline elasticity and the important role of boundary conditions. To better understand the dynamics and rheology of active suspensions, a kinetic model incorporating liquid crystalline elasticity is necessary.

In this work, we generalize the kinetic model presented by Saintillan [6] to incorporate hydrodynamic interactions. Our aim is to provide a systematic study the dynamics and rheology of active suspensions by carrying out a complete exploration of the phase space formed by the three most important physical characteristics of the system: the swimmer type and activity, their flow alignment behavior, and the boundary conditions. Our analysis confirms the recent experimental results on Bacillus subtilis [18] and Chlamydomonas [19].

II. MODEL FORMULATION

For a rigid spheroidal suspension in a fluid, Jeffery [24] first calculated the velocity of its axis of revolution $\mathbf{m}$ as follows,

$$\dot{\mathbf{m}} = \Omega \cdot \mathbf{m} + a[\mathbf{D} \cdot \mathbf{m} - D : \mathbf{mmm}] \tag{1}$$

where $\Omega = \frac{1}{2}(\nabla \mathbf{v} - \nabla \mathbf{v}^T)$ and $\mathbf{D} = \frac{\mathbf{1}}{\mathbf{2}}(\nabla \mathbf{v} + \nabla \mathbf{v}^{\mathbf{T}})$ are the rate-of vorticity and the rate-of-strain tensors, respectively, and a is the shape parameter defined by $a = \frac{r^2-1}{r^2+1}$ where r is the ratio of the rod length or plate thickness to

the diameter, $0 < a \leq 1$ corresponds to a rodlike particle and $-1 \leq a < 0$ for a disclike particle.

In our model, we assume that all particles are of the same rigid spheroidal configuration immersed in viscous fluid. The evolution of a suspension particle is described by a continuity equation for the orientation distribution function $f(\mathbf{x}, \mathbf{m}, t)$ of rigid spheroidal particles with axis of symmetry $\mathbf{m}$ (i.e., the particle director) on the unit sphere S^2 at position $\mathbf{x}$, which satisfies the Smoluchowski equation [20].

$$\frac{\partial f}{\partial t} = Dr\mathcal{R} \cdot (\mathcal{R}f + \frac{1}{kT} f\mathcal{R}U) - \mathcal{R} \cdot [\mathbf{m} \times \dot{\mathbf{m}} f], \qquad (2)$$

where $\mathcal{R} = \mathbf{m} \times \partial/\partial\mathbf{m}$ is the rotational gradient operator, D_r is the rotational diffusion rate, k is the Boltzmann constant, T is the temperature, U is the Marrucci-Greco mean-field nematic potential, defined by

$$U = -\frac{3}{2} NkT(\mathbf{M} + \frac{\mathcal{L}^2}{24}\Delta\mathbf{M}) : \mathbf{mm}, \qquad (3)$$

where N specifies the strength of the nematic (excluded volume) potential and $\mathcal{L}$ is a characteristic length for particle interaction, $\mathbf{M} = \int_{||\mathbf{m}||=1} \mathbf{mm} f d\mathbf{m}$ is the second moment of $\mathbf{m}$ with respect to PDF, the deviatoric part of $\mathbf{M}$

$$\mathbf{Q} = \mathbf{M} - \mathbf{I}/3. \qquad (4)$$

is called the orientation tensor which is the traceless normalization of the second moment $\mathbf{M}$. $\mathbf{Q}$ and $\mathbf{M}$ share an orthonormal frame of principal axes, called the directors in the nematic liquid literature.

Once the orientation distribution f is known by solution of equation, it can be used to evaluate the stress tensor in the suspension.

We shall see that the stress tensor is expressed in terms of moments of PDF. Hence, instead of solving Eq. (2), we will seek the solutions of $\mathbf{M}$ or the orientation tensor $\mathbf{Q} = \mathbf{M} - \frac{\mathbf{I}}{3}$ whose governing equation can be derived from Eq. (2) by multiplying both sides by $\mathbf{mm}$ and integrating over the unit sphere.

$$\begin{aligned} &\dot{\mathbf{M}} = a[\mathbf{D} \cdot \mathbf{M} + \mathbf{M} \cdot \mathbf{D} - 2\mathbf{D} : \mathbf{M}_4] - 6DrF(\mathbf{M}), \\ &F(\mathbf{M}) = \mathbf{Q} - \mathbf{N}(\mathbf{M} \cdot \mathbf{M} - \mathbf{M} : \mathbf{MM})] \\ &+ \frac{N\mathcal{L}^2}{48}[\Delta\mathbf{M} \cdot \mathbf{M} + \mathbf{M} \cdot \Delta\mathbf{M} - 2\Delta\mathbf{M} : \mathbf{M_4} \end{aligned} \qquad (5)$$

where $\dot{\mathbf{M}} = \frac{d\mathbf{M}}{dt} - \Omega \cdot \mathbf{M} + \mathbf{M} \cdot \Omega$ and $\frac{d\mathbf{M}}{dt}$ denotes the material derivative of $\mathbf{M}$. To close the system, we apply the following quadratic closure approximation $\mathbf{M_4} = \mathbf{MM}$.

Under macroscopic flow, the evolution Eq. (5) couples to the the Navier-Stokes equation through the stress tensor. Following Doi and Edwards [20] we write the stress as the sum which can be divided into a elastic, a viscous and an active part.

$$\tau = \tau^e + \tau^v + \tau^a \qquad (6)$$

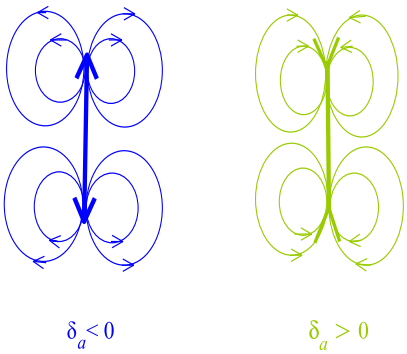

FIG. 1: The dipolar flow fields surrounding a extensile (left) and a contractile (right) particle. The vertical arrows represent the director field, which is along the rod axis for rodlike particles and perpendicular to the disk plane for disclike particles.

The first two contributions also arise with passive particles and were obtained previously as [21].

$$\begin{aligned} \tau^e = 3a\nu kTF(\mathbf{M}) - \frac{\nu\mathbf{kTN}\mathcal{L}^\mathbf{2}}{\mathbf{32}}[\mathbf{2}(\mathbf{\Delta M} \cdot \mathbf{M} \\ -\mathbf{M} \cdot \Delta\mathbf{M}) - \nabla\mathbf{M} : \nabla\mathbf{M} - \nabla\nabla\mathbf{M} : \mathbf{M}] \end{aligned} \qquad (7)$$

$$\tau^v = 2\eta_s \mathbf{D} \qquad (8)$$

where ν is the suspension number density and η_s is the viscosity of the suspending liquid.

The component of the stress resulting from the permanent dipole can be expressed as [1, 5],

$$\tau^a = \delta_a(\mathbf{M} - \tfrac{1}{3}\mathbf{I}) \qquad (9)$$

The sign of δ_a determines whether the dipolar flow field generated by the swimming suspension is extensile ($\delta_a < 0$) or or contractile ($\delta_a > 0$, as illustrated in Fig. 1. In the swimmer literature, the former situation describes "pushers", i.e., most bacteria (e.g., E. Coli), while the latter corresponds to "pullers" (e.g., Chlamydomonas).

We consider shear flow between two parallel plates located at $y = \pm h$ and moving with velocity $\mathbf{v} = (\pm v_0, 0, 0)$, respectively, in Cartesian coordinates (x, y, z). We assume strong particle anchoring at the plates given by the quiescent nematic equilibrium of the orientation tensor (the deviatoric part of the structure tensor) i.e., $\mathbf{Q} = \mathbf{Q_0} = \mathbf{s_0}(\mathbf{n_0 n_0} - \frac{\mathbf{I}}{\mathbf{3}})$ where $s_0 = \frac{1}{4}[1 + 3\sqrt{1 - \frac{8}{3N}}]$, $\mathbf{n_0} = (\cos\varphi_\mathbf{0}, \sin\varphi_\mathbf{0}, \mathbf{0})$, and the initial director is $\mathbf{n_0}$. The uniaxial director $\mathbf{n_0}$ is arbitrary for quiescent phases; this degeneracy is broken experimentally by mechanical or chemical plate preparations. Fig. 2 depicts the cross section of the shear

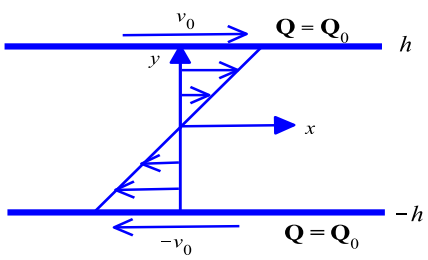

FIG. 2: Plane shear flow geometry. Nonslip boundary conditions for the velocity and boundary anchoring for the orientation tensor is assumed to equal to its quiescent nematic equilibrium value.

flow on the (x,y) plane. Variations in the direction of flow (x) and primary vorticity direction (z), and transport in the vertical (y) direction are suppressed. We nondimensionalize the system using the length scale the gap half-width (h), time scale $t_0 = \frac{1}{D_r^0}$ and stress scale $\tau_0 = 3\nu kT$, then we have four dimensionless parameters: $Re = \frac{\rho h^2}{3\nu k T t_0^2}, Er = \frac{8h^2}{N\mathcal{L}^2}, \delta = \frac{\delta_a}{\tau_0}, \eta = \frac{\eta_s}{t_0\tau_0}$. The dimensionless plate velocity is defined by the Deborah number, $De = \frac{v_0}{Drh}$.

We hereafter use only dimensionless scales and variables in all equations, solutions, and figures. The boundary conditions for the scaled velocity $\mathbf{v}$ and the orientation tensor $\mathbf{Q}$ are

$$\begin{aligned} &\mathbf{v}|_{y=\pm 1} = (\pm De, 0, 0), \\ &\mathbf{Q}|_{y=\pm 1} = \mathbf{Q}_0 \end{aligned} \tag{10}$$

We model a uniform plate anchoring condition, either parallel to the flow direction, called tangential anchoring, or perpendicular to the shearing plates, called homeotropic (or normal) anchoring. The majority of the symbolic and numerical calculations presented in this paper were performed using the software MAPLE 12 by Waterloo Maple Inc. The values of parameters used in this paper are $N = 4$, $Er = 2000$ and $\eta = 0.1$.

III. WEAK STEADY SHEAR FLOWS AND STABILITY ANALYSIS

We seek asymptotic solutions of the governing system of equations with the boundary conditions given by (10). We employ a biaxial representation of the orientation tensor

$$\mathbf{Q} = s\left(\mathbf{nn} - \frac{1}{3}\mathbf{I}\right) + \beta\left(\mathbf{n}^\perp\mathbf{n}^\perp - \frac{1}{3}\mathbf{I}\right), \tag{11}$$

where (s, β) are two order parameters measuring the birefringence relative to the optical axes (also called directors) $\mathbf{n}$ and $\mathbf{n}^\perp$ confined to the shearing plane (x, y) and parameterized by a director angle φ,

$$\mathbf{n} = (\cos\varphi, \sin\varphi, 0), \qquad \mathbf{n}^\perp = (-\sin\varphi, \cos\varphi, 0), \tag{12}$$

and $\mathbf{I}$ is the 3×3 identity matrix. We propose the solution ansatz

$$v_x = \sum_{k=1}^{\infty} De^k v_x^{(k)}, (\bullet) = \sum_{k=0}^{\infty} (\bullet)_k De^k, \tag{13}$$

$$\varphi = \varphi_0 + \sum_{k=1}^{\infty} \varphi^{(k)} De^k \tag{14}$$

where $(\bullet)$ represents the order parameters s, β, respectively. The solution is sensitive to the choice of boundary conditions, so we present tangential ($\varphi_0 = 0$) and normal ($\varphi_0 = \frac{\pi}{2}$) anchoring conditions separately. We drop the subscript on φ for brevity and use v_x to express $v_x^{(1)}$. The linearized system reduces to

$$\begin{aligned} &\frac{\partial\varphi}{\partial t} = A\frac{\partial^2\varphi}{\partial y^2} + B\frac{\partial v_x}{\partial y}, \\ &Re\frac{\partial v_x}{\partial t} = \frac{\partial\tau_{xy}}{\partial y}, \\ &\tau_{xy} = C\frac{\partial^2\varphi}{\partial y^2} + D\frac{\partial v_x}{\partial y} + s_0\delta\varphi, \end{aligned} \tag{15}$$

where

$$A = \frac{s_0+2}{3Er}, B = \frac{\lambda_L - 1}{2}, C = -\frac{s_0^2}{3Er}B, D = \eta \tag{16}$$

where λ_L is the Leslie tumbling parameter which is defined as $\lambda_L = \frac{a(2+s_0)}{3s_0}$, $|\lambda_L| > 1$ corresponds to flow aligning and $|\lambda_L| < 1$ corresponds to flow tumbling. We note that high aspect ratio rods or platelets tend to align while low aspect ratio ones tend to tumble. Fig. 3 depicts the flow aligning and tumbling regimes for different shapes of spheroids.

The steady state of the system (15) is pretty simple,

$$\begin{aligned} &v_x = \frac{\sinh ry}{\sinh r}, \\ &\varphi = -\frac{B\coth r}{Ar}\left(\frac{\cosh ry}{\cosh r} - 1\right) \end{aligned} \tag{17}$$

where $r = \sqrt{\frac{s_0}{2(AD-BC)}(\lambda_L - 1)\delta}$. It is real (imaginary) if $(\lambda_L - 1)\delta > 0$ (< 0). This shows that the steady state structure of contractile (extensile) systems with $\lambda_L > 1$ are the same as those of extensile (contractile) systems with $\lambda_L < 1$. One can see (17) is hyperbolic (sinusoidal)

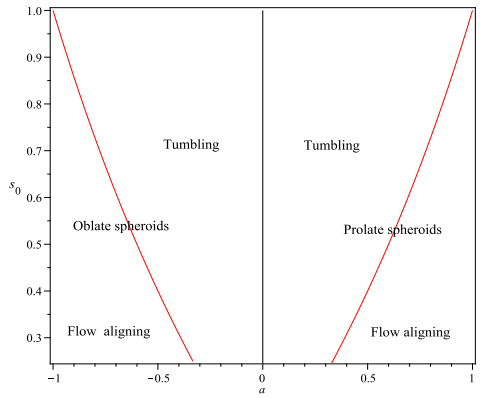

FIG. 3: The flow aligning and tumbling regimes for different shapes of spheroids

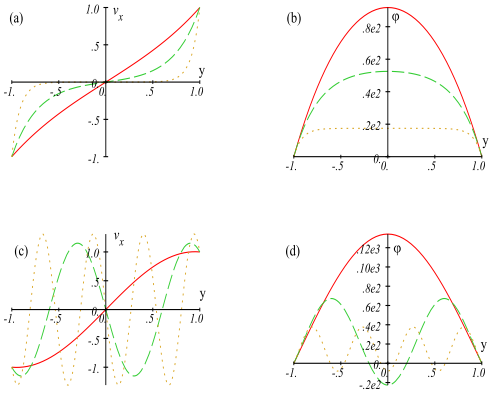

FIG. 4: The typical first order steady states. (a) and (b) depict the velocity and the director profiles for the flow-aligning contractile rodlike particles ($a = 0.9$) with tangentially anchored boundary conditions at different activity : solid, dashed and dotted lines correspond to $\delta = 0.001, 0.01, 0.1$. (c) and (d) depict the velocity and the director profiles for the flow-aligning extensile rodlike particles ($a = 0.9$) with tangentially anchored boundary conditions at different activity : solid, dashed and dotted lines correspond to $\delta = -0.002, -0.02, -0.1$.

if $(\lambda_L - 1)\delta > 0$ (< 0) and as $\delta \to 0$, the steady state of a passive nematics will be recovered [22]. However at high activity, the story will be totally changed: when $(\lambda_L - 1)\delta > 0$, the flow velocity is zero and the director angle is a constant away the plates, which is akin to permeation in passive cholesteric liquid crystals [23]. Fig. 4(a) and Fig. 4(b) depicts these typical velocity and director profiles for flow-aligning/contractile particles. When $(\lambda_L - 1)\delta < 0$, both the flow velocity and the director angle are spatially oscillatory. We notice that this periodic structure occurs at high activity, which perhaps can only happen at the concentration regime close to smectic transition. Fig. 4(c) and Fig. 4(d) depicts these typical velocity and director profiles for flow-aligning/contractile particles.

The transient solution for v_x and φ (the difference between the time-dependent solution and the steady state) obeys the same homogeneous linear partial differential equations but satisfies a zero boundary condition. Its behavior dictates the stability of the steady state within the asymptotic balance model: the steady state is asymptotically stable if the transient solution vanishes as $t \to \infty$. By the energy method, we can prove the following theorem.

Theorem: The steady state is stable for tangential anchoring if $(\lambda_L - 1)\delta > 0$. In other cases, the steady state is stable at low activity.

Proof We note that $A > 0$, $D > 0$, $BC < 0$ and $AD - BC > 0$. In the following proof, we drop the superscripts on φ and v_x. Extending $(15)_1$ to the boundary and accounting for the boundary condition $\varphi(-1, t) = \varphi(1, t) = 0$, we have

$$(A\frac{\partial^2 \varphi}{\partial y^2} + B\frac{\partial v_x}{\partial y})|_{y=\pm 1} = 0. \tag{18}$$

We introduce a nonnegative functional

$$I(t) = \int_{-1}^{1} [\gamma_1 \varphi_y^2 + \gamma_2 Re v_x^2 + \gamma_3 \varphi^2] dy \tag{19}$$

with $\gamma_1 > 0$, $\gamma_2 > 0$ and $\gamma_3 > 0$.

If $B\delta > 0$, i.e., B and δ have same signs. We choose $\gamma_1 = |C|$, $\gamma_2 = |B|$ and $\gamma_3 = s_0|B|\frac{\delta}{B}$ and integrating by parts, the time derivative of the nonnegative functional can be estimated:

$$\begin{aligned} \frac{dI(t)}{dt} &= -2\int_{-1}^{1} [\gamma_1 A \varphi_{yy}^2 + (\gamma_1 B + \gamma_2 C)\varphi_{yy} v_{x,y} \\ &+ \gamma_2 D v_{x,y}^2 + \gamma_3 A \varphi_y^2 + (\gamma_3 B - s_0 \gamma_2 \delta)\varphi_y v_x] dy \\ &= -2\int_{-1}^{1} [|C| A \varphi_{yy}^2 + |B| D v_{x,y}^2 + A s_0 |B| \tfrac{\delta}{B} \varphi_y^2] dy < 0. \end{aligned} \tag{20}$$

This shows that the steady solution of the system is stable.

If $B\delta < 0$, i.e., B and δ have same signs. Choosing $\gamma_1 = |C|$, $\gamma_2 = |B|$ and $\gamma_3 = 0$, then

$$\begin{aligned} \frac{dI(t)}{dt} &= -2\int_{-1}^{1} [|C| A \varphi_{yy}^2 + |B| D v_{x,y}^2] dy \\ &+ 2\delta s_0 |B| \int_{-1}^{1} \varphi_y v_x] dy < 0. \end{aligned} \tag{21}$$

The inequality is based on small values of δ and the proof is complete.

The rheological property of interest is the apparent viscosity defined by $\eta_{app} = \frac{\tau_{xy}}{2F}$ [25–27] where $F = \int_0^1 v_x(y) dy$ is the flow rate per unit length and

$$\tau_{xy} = \frac{B s_0 \delta \coth r}{Ar} \tag{22}$$

is the shear stress, which is a constant at this order across the shear cell. The resulting apparent viscosity is given by

$$\eta_{app} = \frac{B s_0 \delta \cosh r}{2A(\cosh r - 1)} \tag{23}$$

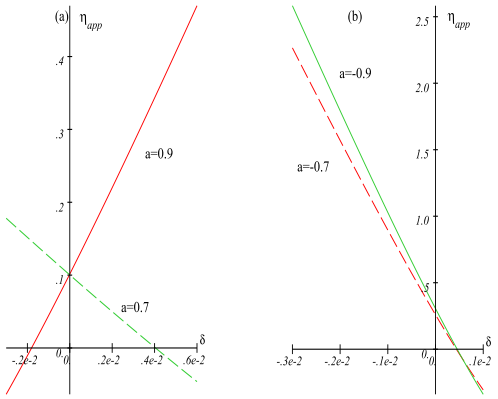

FIG. 5: The apparent viscosity as functions of the activity. (a) and (b) are for rodlike and disclike particles, respectively.

We first note that the shear viscosity of passive nematics [22] will be recovered as expected as $\delta \to 0$. When r is real,i.e., $(\lambda_L - 1)\delta > 0$, η_{app} increases as δ increases, which means η_{app} is thickened by δ. When r is imaginary,i.e., $(\lambda_L - 1)\delta < 0$, η_{app} is not monotonic. However, we find, if $|\delta| < \frac{\pi^2(4(s_0+2)+s_0(\lambda_L-1)^2)}{6s_0 Er|\lambda_L-1|}$, η_{app} is a decreasing fuction of δ, which means η_{app} is thinned by the activity δ. A negative apparent viscosity is found for flow-aligning/extensile and tumbling/contractile rodlike particles and contractile/disclike particles at high activity. These results confirm the previous predictions by Hatwalne et al [1] and Saintillan [6] and observed in [18, 19].

Fig. 5 shows the apparent viscosity versus the activity for both contractile and extensile rodlike and disclike particles. We can see that for flow-aligning/contractile rodlike particles (a) and extensile/disclike particles (b), the systems are always thickened by the activity; for flow-aligning/extensile and tumbling/ contractile rodlike particles (a) and contractile/disclike particles (b), the systems are thinned by the low activity but are thickened by the high activity. The figure also shows that a negative apparent viscosity occurs for flow-aligning/extensile and tumbling/ contractile rodlike particles (a) and contractile/disclike particles (b).

For homotropic anchoring condition, we note that the governing system (15) admits a symmetry: $(a, \delta, \varphi) \to (-a, -\delta, \pi/2+\varphi)$. This property implies the steady states with $\varphi_0 = \pi/2$ can be obtained directly from the steady states with $\varphi_0 = 0$ by changing $(a, \delta) \to (-a, -\delta)$. So is the apparent formula. We omit the detail and summarize our main results in Fig. 6.

IV. CONCLUSION

We have studied the steady structure and rheological behavior of a thin film of active suspension of rigid ellipsoids. We find the shape of a particle plays an important role in controlling the flow and rheological behavior, which is consistent with the previous predictions by [1, 5, 6] and the experimental results on flow-aligning rodlike particles [18, 19]. Our results include both rodlike and disclike particles, we look forward to tests of all the predictions in experiments on active systems.

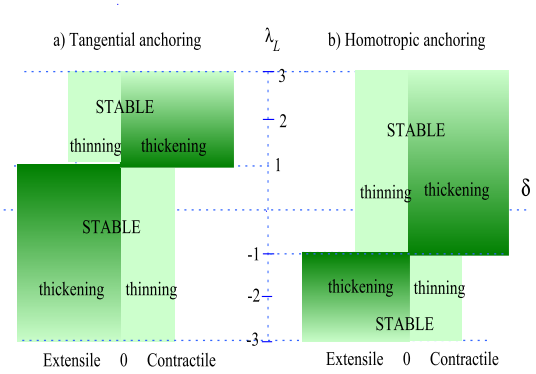

FIG. 6: Phase diagram in the (δ, λ_L) plane. Steady state stable regions and apparent viscosity thinning/thickening regions. Steady spontaneous oscillatory states arises in unstable regions (unshaded).

Acknowledgements: This research is supported in part by Fayetteville State University Faculty Development Mini-grants.

[1] Y. Hatwalne et al, Phys. Rev. Lett. 92, 118191 (2004).
[2] T. B. Liverpool, M. C. Marchetti, Phys. Rev. Lett. 97, 268101 (2006).
[3] D. Marenduzzo, E. Orlandini, J. M. Yeomans, Phys. Rev. Lett. 98, 118102 (2007)
[4] L. Giomi, M. C. Marchetti and T. B. Liverpool, Phys. Rev. Lett. 101, 198101 (2008).
[5] L. Giomi et al, Phys. Rev. E 81, 051908 (2010).
[6] D. Saintillan, Exp. Mech. in press, 2010.
[7] S. A. Edwards and J. M. Yeomans, Europhys. Lett. 85, 18008 (2009).
[8] R. Voituriez, J. F. Joanny and J. Prost, Europhys. Lett. 70, 118102 (2005).
[9] C. Dombrowski et al , Phys. Rev. Lett. 93, 098103 (2004).
[10] D. Saintillan and M. J. Shelley, Phys. Rev. Lett. 100, 178103 (2008).
[11] F. Neédélec, T. Surrey, and E. Karsenti, Curr. Opin. Cell Biol. 15, 118 (2003).
[12] H. Gruler, U. Dewald, and M. Eberhardt, Eur. Phys. J. B 11, 187 (1999).

[13] M. J. Kim and K. S. Breuer, J. Fluids Eng. 129, 319 (2007).
[14] P. D. Olmsted, Rheol. Acta 47, 283 (2008).
[15] B. Chakrabarty, M. Das, C. Dasgupta, S. Ramaswamy, and A. K. Sood, Phys. Rev. Lett. 92, 055501 (2004).
[16] D. Kaiser, Current Biology, 17, R561 (2007).
[17] M. E. Cates et al, Phys. Rev. Lett. 101, 068102 (2008).
[18] A. Sokolov and S. Aranson, Phys. Rev. Lett. 103, 148101 (2009).
[19] S. Rafaï, L. Jibuti, and P. Peyla, Phys. Rev. Lett. 104, 098102 (2010).
[20] M. Doi, S. F. Edwards, The Theory of Polymer Dynamics, Oxford University Press (Clarendon), London-New York (1986).
[21] Q. Wang, J Chem. Phys. 116(20), 9120 (2002).
[22] Z. Cui et al, SIAM J. Appl. Math. 66 (4), 1227 (2006).
[23] Z. Cui, M.C. Calderer,and Q. Wang, Discrete and Continuous Dynamical Systems-Series B, 6(2), 291, (2006).
[24] G. B. Jeffery, Proc R Soc Lond Ser A 102, 161 (1922).
[25] F. A. Morrison, Understanding Rheology, Oxford University Press, New York, 458 (2001).
[26] A.D. Rey, J. Rheol. 46 (1), 225 (2002)
[27] Z. Cui, Communications in Mathematical Sciences, in press, 2010.